Effective L-shell fluorescence yields for sodiumlike and neonlike low-lying autoionizing states

Mau Hsiung Chen

High Temperature Physics Division, Lawrence Livermore National Laboratory, Livermore, California 94550

(Received 7 March 1989)

The statistically averaged L-shell fluorescence yields for the doubly excited $3l3l'$ and $3l4l'$ configurations of Na- and Ne-like ions have been calculated for ions with $18 \leq Z \leq 92$ using Dirac-Fock wave functions. The average $n=3 \rightarrow 2$ radiative rates and Auger rates for the $3l3l'$ states of the Na-like ions scale as $Z^{5.1}$ and $Z^{0.71}$, respectively. The procedure for calculating the average fluorescence yield as ratio between the average x-ray rate and average total decay rate underestimates the average fluorescence yield by as much as a factor of 3 for low-Z ions and overestimates by 50% for heavy ions. Inclusion of $E2$ transitions leads to a 25% increase in the average fluorescence yield for the Na-like $3l3l'$ states at $Z=80$.

I. INTRODUCTION

In heavy-ion–atom collisions, multiple ionization has been found to be more probable than single ionization.[1] Most studies concerning multiple vacancies are based on measurements of x-ray spectra. The x-ray fluorescence yields of defect configurations are required to convert x-ray yields into ionization cross sections. Sodiumlike and neonlike doubly excited $3l3l'$ and $3l4l'$ states are some of the most important autoionizing states encountered in laboratory produced plasmas. They contribute to the dielectronic recombination processes and produce L x-ray satellites which may be useful in plasma diagnostics.

The early calculations of average fluorescence yields $\bar{\omega}$ for multiple-vacancy atoms[2–4] were based on the formula

$$\bar{\omega}_a = \frac{\bar{\Gamma}_x}{\bar{\Gamma}_x + \bar{\Gamma}_A} . \tag{1}$$

Here, $\bar{\Gamma}_x$ and $\bar{\Gamma}_A$ are the statistically averaged x-ray and Auger rates for the relevant configuration. Equation (1) has also been frequently used to compute the x-ray branching ratio in calculations of dielectronic recombination cross sections or rate coefficients.[5,6] However, Eq. (1) has been shown to underestimate significantly the average fluorescence yields, especially for few-electron ions.[7–9] The reason for this difficulty can be traced to the fact that Eq. (1) ignores the possible closure of Auger and x-ray channels due to the angular momentum and parity selection rules.

To remedy this deficiency, the effective fluorescence yield for a configuration should be evaluated as a weighted sum of the fluorescence yield for each multiplet state:[10]

$$\bar{\omega}_d = \frac{\sum_i P(S_i L_i J_i)\,\omega(S_i L_i J_i)}{\sum_i P(S_i L_i J_i)} , \tag{2}$$

where $P(S_i L_i J_i)$ is the relative population of the initial state, and

$$\omega(S_i L_i J_i) = \frac{\Gamma_x(S_i L_i J_i)}{\Gamma_x(S_i L_i J_i) + \Gamma_A(S_i L_i J_i)} . \tag{3}$$

Here, $\Gamma_x(S_i L_i J_i)$ and $\Gamma_A(S_i L_i J_i)$ are the total x-ray and Auger rates of the multiplet state $S_i L_i J_i$, respectively. For statistical population of initial states we have $P(S_i L_i J_i) = 2J_i + 1$.

The average L-shell fluorescence yields for $_{18}$Ar, $_{17}$Cl, and $_{16}$S with multiple M-shell vacancies have been calculated using Hartree-Slater wave functions.[7,11] In this paper, we report on the calculations of the effective L-shell fluorescence yields for the $2l^{-1}3l'3l''$ and $2l^{-1}3l'4l''$ configurations of the neonlike and sodiumlike ions using Dirac-Fock wave functions. Here, $2l^{-1}$ means an electron missing in the $2l$ subshell. The calculations were carried out for ions with atomic number $18 \leq Z \leq 92$. Trends of the average Auger rates, radiative rates, and fluorescence yields, and the differences between the effective fluorescence yields calculated from Eqs. (1) and (2) are discussed in Sec. III and the calculational procedure is described in Sec. II.

II. CALCULATIONAL PROCEDURE

The Auger transition probability is calculated from perturbation theory.[12] The transition rate from the initial state i to the final state f is given in frozen-orbital approximation by

$$T = \frac{2\pi}{\hbar} \left| \left\langle \Psi_f \left| \sum_{\substack{\alpha,\beta \\ \alpha<\beta}} V_{\alpha\beta} \right| \Psi_i \right\rangle \right|^2 \rho(\varepsilon) . \tag{4}$$

Here, $\rho(\varepsilon)$ is the energy density of final states, and the two-electron interaction operator $V_{\alpha\beta}$ is taken to be the Coulomb interaction.

The general expressions for the state-to-state Auger transition rates involving many open-shell systems have been derived by McGuire.[13] If one assumes that the radial matrix element is independent of the multiplet structure, the expression for the multiplet Auger transition[13] can be summed and averaged to give the configuration-averaged Auger rate. For transitions involving nonequivalent electrons with j-j configuration

$$[(n_1j_1)^m(n_3j_3)^n(n_4j_4)^p \rightarrow (n_1j_1)^{m+1}(n_3j_3)^{n-1}(n_4j_4)^{p-1}\epsilon j_2 ,$$

the statistically averaged Auger rate is given by[13]

$$\overline{\Gamma}_A=(2j_1+1-m)\frac{np}{(2j_3+1)(2j_4+1)}\Gamma_A^0 , \quad (5)$$

where Γ_A^0 is the full-shell rate for an atom with one inner-shell vacancy and otherwise closed-shell configuration. The expression for the full-shell rate for relativistic calculation can be found in Ref. 14.

For Auger transitions

$$(n_1j_1)^m(n_3j_3)^n \rightarrow (n_1j_1)^{m+1}(n_3j_3)^{n-2}\epsilon j_2$$

with equivalent active electrons, the j-j configuration average Auger rate can be written as

$$\overline{\Gamma}_A=(2j_1+1-m)\frac{n(n-1)}{(2j_3+1)(2j_3)}\Gamma_A^0 . \quad (6)$$

In Eqs. (5) and (6), m, n, and p are the numbers of electrons in j_1, j_3, and j_4 subshells, respectively, and ϵj_2 represents the continuum electrons.

For radiative transition

$$(n_1j_1)^m(n_2j_2)^n(\alpha_R J_R) \rightarrow (n_1j_1)^{m+1}(n_2j_2)^{n-1}(\alpha_R J_R) ,$$

the statistically averaged radiative rate for the j-j configuration is given by[15]

$$\overline{\Gamma}_x=(2j_1+1-m)\frac{n}{2j_2+1}\Gamma_x^0 . \quad (7)$$

Here, m and n are the numbers of electrons in j_1 and j_2 subshells, respectively. The full-shell rate Γ_x^0 for an atom with one inner-shell vacancy and otherwise closed-shell configuration is given in Ref. 15.

There are 237 j-j coupled states for the Na-like $2l^{-1}3l'3l''$ configurations and many more for the $2l^{-1}3l'4l''$ and Ne-like $2l^{-2}3l'3l''$ configurations. The detailed state-to-state Auger and radiative rates for each of the j-j coupled states were calculated using the multiconfiguration Dirac-Fock model (MCDF).[16] The term-dependent transition rates for some of the ions investigated in the present work have been used to calculate the dielectronic recombination rate coefficients.[17] A detailed calculational procedure for the term-dependent Auger and radiative rates using MCDF model has been presented in Ref. 18.

In the present work, the atomic energy levels and bound-state wave functions were evaluated using the MCDF model in the average-level scheme.[16] The calculations were carried out in intermediate coupling and included configuration interaction within the same complex. These term-dependent Auger and radiative rates were used to compute the fluorescence yield for each autoionizing state according to Eq. (3). The statistically averaged fluorescence yields $\overline{\omega}_d$ were then determined according to Eq. (2). The Dirac-Fock orbital wave functions obtained for the detailed calculations were also employed to calculate the average Auger rates $\overline{\Gamma}_A$ and radiative rates $\overline{\Gamma}_x$ using Eqs. (6) and (7), respectively. The average fluorescence yields $\overline{\omega}_a$ were then calculated according to Eq. (1).

III. RESULTS AND DISCUSSION

The average L-shell Auger $\overline{\Gamma}_A$ and radiative rates $\overline{\Gamma}_x$ for the Na- and Ne-like ions are shown in Figs. 1 and 2. For the Na-like doubly excited $3l3l'$ states, the Z dependences of the average $n=3\rightarrow2$ radiative rates and Auger rates in $\sec^{-1}$ were determined by least-squares fit to the theoretical data; they are given by

$$\overline{\Gamma}_x=7.03\times10^4Z^{5.1}$$

and

$$\overline{\Gamma}_A=1.6\times10^{12}Z^{0.71} .$$

For the Ne-like doubly excited $3l3l'$ configurations, we have

$$\overline{\Gamma}_x=9.76\times10^5Z^{4.6}$$

and

$$\overline{\Gamma}_A=3.12\times10^{13}Z^{0.15} .$$

The Auger rate stays almost constant as Z increases, while the radiative rate increases by more than three orders of magnitude as Z increases from 18 to 79. For the $3l4l'$ doubly excited configurations, similar scaling laws

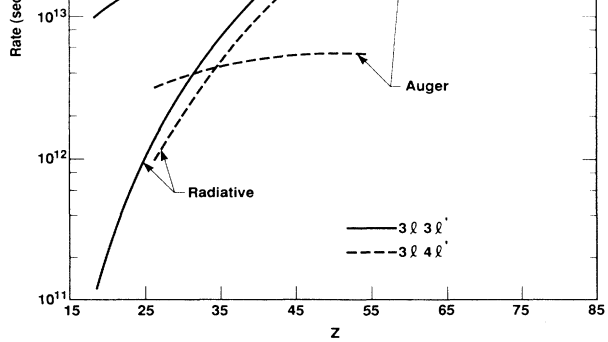

FIG. 1. Average L-shell Auger and radiative rates for the Na-like ions as functions of atomic number. The solid curves indicate the results for the $3l3l'$ configurations. The dashed curves represent the values for the $3l4l'$ configurations.

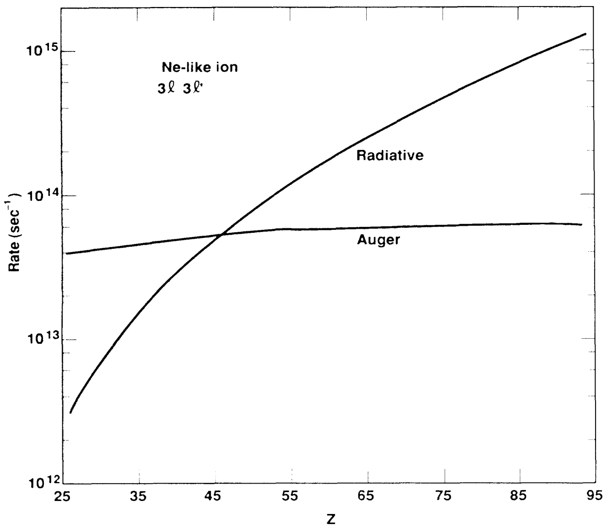

FIG. 2. Average L-shell Auger and radiative rates for the $3l3l'$ configurations of the Ne-like ions.

have been found for the average L-shell Auger and radiative rates.

In a simple hydrogenic approximation, the x-ray energy is proportional to Z^2 and the electric dipole matrix element scales as $1/Z$. Thus the radiative rate scales as Z^4. However, the hydrogenic scaling rule may change due to the effects of electron screening and relativity. In the present work, the $n=3-2$ x-ray energy for the Na-like $3l3l'$ states has been found to scale as $Z^{2.3}$, which results in a slightly higher Z dependence in radiative rate than the hydrogenic approximation.

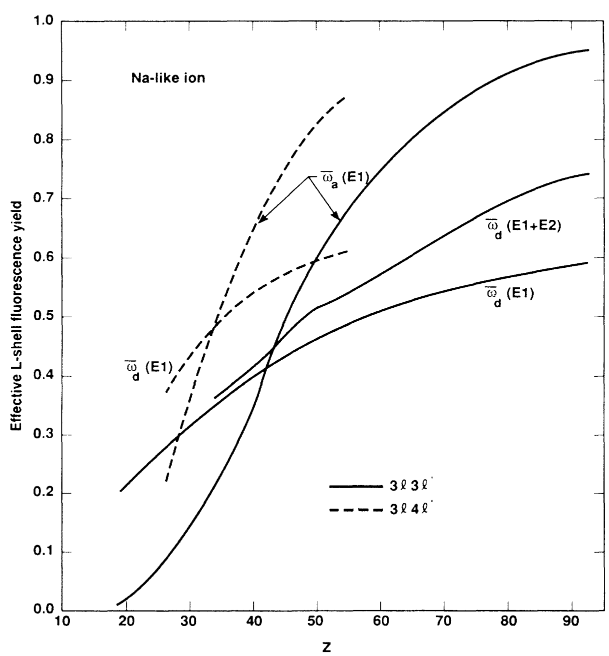

FIG. 3. Effective L-shell fluorescence yields for the Na-like ions. The solid curves display the results for the $3l3l'$ configurations and the dashed curves indicate the predictions for the $3l4l'$ configurations.

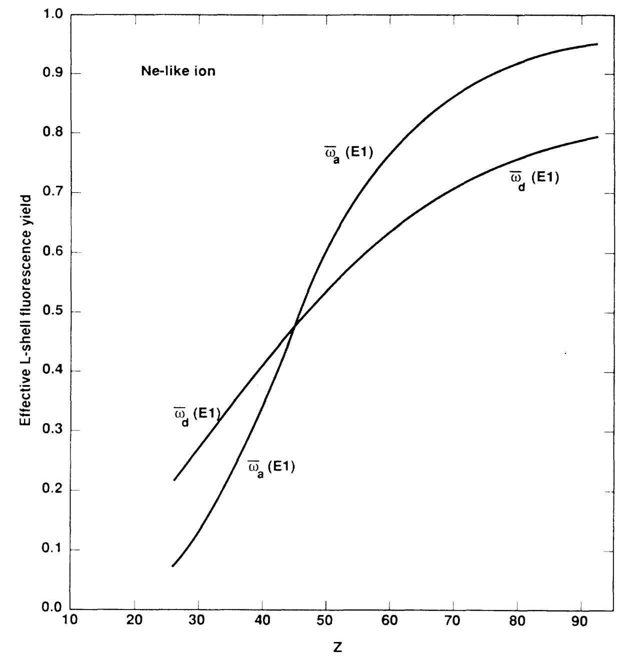

FIG. 4. Effective L-shell fluorescence yields for the $3l3l'$ configurations of the Ne-like ions.

The effective L-shell fluorescence yields $\overline{\omega}_a$ and $\overline{\omega}_d$ are compared in Figs. 3 and 4. For the Na- and Ne-like $3l3l'$ configurations, the average fluorescence yield $\overline{\omega}_a$ calculated according to Eq. (1) underestimates the fluorescence yield at low Z by as much as a factor of 3 and overestimates for high-Z ions by 50%. For the mid-Z ions, $\overline{\omega}_a$ agrees quite well with $\overline{\omega}_d$. Similar behavior has been found for the $\overline{\omega}_a$ and $\overline{\omega}_d$ of the Na-like $3l4l'$ doubly excited configurations. The Z dependence of the quantities $\overline{\omega}/(1-\overline{\omega})$ were determined by least-squares fit to the theoretical values. For the Na-like $3l3l'$ configurations, they are given by

$$\frac{\overline{\omega}_d}{1-\overline{\omega}_d}=1.17\times10^{-2}Z^{1.08}$$

and

$$\frac{\overline{\omega}_a}{1-\overline{\omega}_a}=2.82\times10^{-8}Z^{4.53}\ .$$

For the Ne-like $3l3l'$ configurations, similar expressions were obtained:

$$\frac{\overline{\omega}_d}{1-\overline{\omega}_d}=3.80\times10^{-4}Z^{2.06}$$

and

$$\frac{\overline{\omega}_a}{1-\overline{\omega}_a}=5.97\times10^{-8}Z^{4.34}\ .$$

The electric quadrupole transition ($E2$) contributes significantly to the average fluorescence yield for heavy ions. The inclusion of $E2$ transitions increases the average L-shell fluorescence yield $\bar{\omega}_d$ by 10% at $Z=45$ and 25% at $Z=80$ (see Fig. 3).

It is rather tempting to employ Eqs. (1) and (5)–(7) to calculate the average fluorescence yields for multiple-vacancy atoms because of their simplicity. However, one should be aware that in some cases the use of Eq. (1) can lead to serious errors.

ACKNOWLEDGMENTS

This work was performed under the auspices of the U. S. Department of Energy by the Lawrence Livermore National Laboratory under Contract No. W-7405-ENG-48.

[1]P. Richard, in *Atomic Inner-Shell Processes,* edited by B. Crasemann (Academic, New York, 1975), p. 73.

[2]F. P. Larkins, J. Phys. B **4**, L29 (1971).

[3]R. J. Fortner, R. C. Der, T. M. Kavanagh, and J. D. Garcia, J. Phys. **B 5**, L73 (1972).

[4]C. P. Bhalla and M. Hein, Phys. Rev. Lett. **30**, 39 (1973).

[5]K. LaGattata and Y. Hahn, Phys. Rev. A **27**, 1675 (1983).

[6]D. C. Griffin, M. S. Pindzola, and C. Bottcher, Phys. Rev. A **31**, 568 (1985).

[7]M. H. Chen and B. Crasemann, Phys. Fenn. Suppl. S1 **9**, 250 (1974); Phys. Rev. A **10**, 2232 (1974).

[8]M. H. Chen, B. Crasemann, and D. L. Matthews, Phys. Rev. Lett. **34**, 1309 (1975).

[9]C. P. Bhalla, Phys. Rev. A **12**, 122 (1975); J. Phys. B **8**, 1200 (1975).

[10]M. H. Chen, in *Atomic Inner-Shell Physics,* edited by B. Crasemann (Plenum, New York, 1985), p. 31.

[11]M. H. Chen and B. Crasemann, Phys. Rev. A **12**, 710 (1975); **16**, 1495 (1977).

[12]W. Bambynek *et al.*, Rev. Mod. Phys. A **4**, 716 (1972).

[13]E. J. McGuire, Ref. 1, p. 293.

[14]M. H. Chen *et al.*, Phys. Rev. A **19**, 2253 (1979).

[15]J. H. Scofield, Phys. Rev. **179**, 9 (1969).

[16]I. P. Grant *et al.*, Comput. Phys. Commun. **21**, 207 (1980).

[17]M. H. Chen, Phys. Rev. A **34**, 1073 (1986).

[18]M. H. Chen, Phys. Rev. A **31**, 1449 (1985).